HHS Public Access

Author manuscript

Science. Author manuscript; available in PMC 2018 February 25.

Published in final edited form as:

Science. 2017 August 25; 357(6353): 806–810. doi:10.1126/science.aah5825.

Lactobacillus reuteri induces gut intraepithelial CD4+CD8αα+ T cells

Luisa Cervantes-Barragan[1], **Jiani N. Chai**[1,2], **Ma. Diarey Tianero**[3], **Blanda Di Luccia**[1], **Philip P. Ahern**[4,5], **Joseph Merriman**[6], **Victor S. Cortez**[1], **Michael G Caparon**[6], **Mohamed S Donia**[3], **Susan Gilfillan**[1], **Marina Cella**[1], **Jeffrey I. Gordon**[4,5], **Chyi-Song Hsieh**[1,2], and **Marco Colonna**[1,*]

[1]Department of Pathology and Immunology, Washington University School of Medicine, St Louis, MO 63110

[2]Department of Internal Medicine, Washington University School of Medicine, St Louis, MO 63110

[3]Department of Molecular Biology, Princeton University, Princeton, NJ 08544, USA

[4]Center for Genome Sciences and Systems Biology, Washington University School of Medicine, St. Louis, MO 63110, USA

[5]Center for Gut Microbiome and Nutrition Research, Washington University School of Medicine, St. Louis, MO 63110, USA

[6]Department of Molecular Microbiology, Washington University School of Medicine, St Louis, MO 63110

Abstract

The small intestine contains CD4+CD8αα+ double-positive intraepithelial T lymphocytes (DP IELs), which originate from intestinal CD4+ T cells through downregulation of the transcription factor ThpoK and have regulatory functions. DP IELs are absent in germ-free mice, suggesting that their differentiation depends on microbial factors. We found that DP IEL numbers in mice varied in different vivaria, correlating with the presence of *Lactobacillus reuteri*. This species induced DP IELs in germ-free mice and conventionally-raised mice lacking these cells. *L. reuteri* did not shape DP-IEL-TCR repertoire, but generated indole derivatives of tryptophan that activated the aryl-hydrocarbon receptor in CD4+ T cells, allowing ThPOK downregulation and differentiation into DP IELs. Thus, *L. reuteri* together with a tryptophan-rich diet can reprogram intraepithelial CD4+ T cells into immunoregulatory T cells.

The gut microbiota drives maturation and function of the immune system (1–3). Several bacterial taxa shape the differentiation of naïve T cells: segmented filamentous bacteria (SFB) bias CD4+ T cells towards a Th17 fate (4), Clostridia clusters IV and XIVa promote CD4+ T regulatory cells (Treg) differentiation (5, 6); and *Bacteroides fragilis* (7, 8) and *Faecalibacterium prausnitzii* (9) induce CD4+ T cells that secrete IL-10. The small intestinal

*Correspondence to: Marco Colonna, Department of Pathology and Immunology, Washington University School of Medicine, 660 S. Euclid St Louis, MO 63110. Tel: 314-362-0367; FAX: 314-747-0809; mcolonna@wustl.edu.

The data reported in this manuscript are presented in the main paper and in the supplementary materials.

epithelium contains a unique population of $CD4^+CD8\alpha\alpha^+$ TCR αβ T cells (referred to as double-positive intraepithelial lymphocytes, or DP IELs) (10). These cells have a regulatory function complementary to that of Tregs and promote tolerance to dietary antigens (11). DP IELs originate from lamina propria $CD4^+$ T cells that include but are not limited to Tregs (11). Upon reaching the epithelium, these cells reactivate the $CD8^+$ T cell lineage program through downregulation of Thpok and upregulation of Runx3 and T-bet (12–14). This process is facilitated in part by transforming growth factor-β (TGFβ), retinoic acid (RA), IFN-γ and IL-27 (12, 14). The lack of DP IELs in germ-free (GF) mice (11, 13) indicates that the intestinal microbiota is required for their differentiation, although the bacterial taxa and metabolites required are not known.

We noticed that mice born at one of our vivaria [specialized research facility (SRF)] harbored substantial numbers of DP IELs (DP^+), whereas DP IELs were negligible or absent (DP^-) in mice from another vivarium [Clinical Sciences Research Building (CSRB)] (Fig. 1A). Moreover, DP IELs in SRF mice expressed low levels of the transcription factor Thpok, $Thpok^{lo}$, whereas CSRB mice lacked $CD4^+$ $Thpok^{lo}$ IELs (13), consistent with the observed lack of DP IELs (fig. S1). Thus, the microbiota in SRF mice might contain taxa capable of inducing DP IELs. Consistent with this, DP IELs appeared in CSRB mice after gavage with fecal or ileal microbiota from SRF, but not CSRB animals (Fig. 1B).

Most SRF (DP^+) mice are embryo-rederived using female recipient mice from Charles River (CR) Laboratories and thus acquire a CR microbiota. In contrast, most CSRB (DP^-) mice originate from the Jackson Laboratories (JAX). Thus, taxa present in CR but not JAX mice might induce DP IELs. Indeed, C57BL/6 mice purchased from CR had a DP^+ phenotype, whereas C57BL/6 mice purchased from JAX had a DP^- phenotype (Fig. 1C). DP^+ and DP^- phenotypes were vertically transmissible (Fig. 1D). Moreover, the DP^+ phenotype was laterally transferable from CR to JAX mice by co-housing animals (Fig. 1E) or by colonizing JAX mice with CR-ileal or fecal microbiota (Fig. 1F). Treatment of CR mice with vancomycin, ampicillin, neomycin and metronidazole (VNAM) abrogated DP IELs (Fig. 1G), as did ampicillin and vancomycin only, which target Gram-positive bacteria; neomycin, which targets Gram-negative bacteria, led to a slight increase in DP IELs (Fig. 1H); metronidazole did not affect DP IELs. Thus, DP IELs are induced by neomycin-resistant Gram-positive bacterial taxa.

To define bacterial taxa that induce DP IELs, we sequenced PCR amplicons from 16S ribosomal RNA genes present in the ileum of CR and JAX mice, as well as neomycin-treated and untreated CR animals. Six operational taxonomic units (OTUs) were selectively present in the CR microbiota and were also present or enriched after neomycin treatment (fig. S2A). These OTUs included *Lactobacillus reuteri* and five members of the *Bacteroidales* S24-7 lineage (Fig. 2A, fig. S2A, and Table S1). *L. reuteri* was present in the ileum of CR control mice and CR mice treated with neomycin or metronidazole, but absent in CR mice treated with ampicillin plus vancomycin (fig. S2B).

Two *L. reuteri* strains (WU and 100-23) induced DP IELs after colonization of JAX mice (Fig. 2B), whereas *L. johnsonii, L. murinus* (Fig. 2C), and various *Bacteroides* species (Fig. 2D) did not. As expected, DP IELs were absent throughout the small intestine of GF animals

(11, 13)(Fig. 2E). Concurrent inoculation of GF mice with *L. reuteri* (WU strain) and ileal microbiota from JAX mice induced DP IELs, whereas JAX ileal microbiota alone was ineffective (Fig. 2F). Mono-colonization with *L. reuteri* resulted in a slight increase of DP IELs. As expected, transfer of CR intestinal microbiota induced DP IELs. Thus, *L. reuteri* induces DP IELs, but the presence of other microbes enhances this effect perhaps by expanding the $CD4^+$ T cells in the lamina propria and epithelium.

We next examined how *L. reuteri* induces DP IELs. If *L. reuteri* antigens shape the specificity of DP IELs, these cells would express quasi-clonal TCR αβ repertoires, as shown for SFB-specific Th17 cells (15). Analysis of TCR Vβ expression on DP IELs, CD4 IELs and mesenteric lymph node (MLN) naïve $CD4^+$ T cells showed that TCR Vβ usage of DP IELs resembled that of CD4 IELs, but was different from that of naïve $CD4^+$ T cells (Fig. 3A). In each mouse analyzed, DP IELs exhibited a preferential Vβ usage (> 2-fold compared to MLN), although no enrichment for a specific Vβ pattern was shared by all mice, suggesting mouse-to-mouse variability in DP IEL TCRs (Fig. 3A and B; and fig. S3A). Because the great diversity of polyclonal T cells complicates analysis at the individual TCR level, we analized the TCR α repertoires of DP IELs, CD4 IELs, CD8 IELs, and MLN naïve $CD4^+$ T cells from mice that express a fixed transgenic TCR β chain ($TCli^+$ mice) (16, 17). $Tcli^+$ T cells were very similar in phenotype and frequency to WT T cells (fig. S3B). TCR Renyi diversity profiles showed both decreased diversity (lower entropy at each order) and evidence for increased clonal expansion (greater downward slope) in the repertoires of all three IEL subsets compared to the repertoire of naïve $CD4^+$ T cells (fig. S3C). The TCR α repertoires of CD4 IELs, CD8 IELs, and DP IELs were distinct from those of naïve $CD4^+$ T cells (Fig. 3C), consistent with the expansion of T cell clones in response to specific antigens. Moreover, the TCR α repertoires of DP IELs and CD4 IELs were similar, but distinct from those of CD8 IELs (Fig. 3D and E), corroborating that DP IELs differentiate from CD4 IELs. Although the TCR α repertoires of naïve T cells were similar in all mice analyzed, the TCR α repertoires of DP IELs and CD4 IELs were quite distinct in each mouse (Fig. 3F), suggesting that the specificity of $CD4^+$ IELs and DP IELs is shaped by various environmental and/or self-antigens in each mouse, rather than by a single antigen.

Some bacterial taxa shape T cell differentiation via their physical components (e.g., polysaccharide A (7, 18)), or their metabolic products (e.g., short-chain fatty acids (19–21)). *L. reuteri* releases reuterin (22), and histamine (23), and also has the ability to metabolize tryptophan (L-Trp) to indole derivatives, some of which activate the aryl-hydrocarbon receptor (AhR) in group 3 innate lymphoid cells (ILC3s) (24, 25). Accordingly, culture supernatants of *L. reuteri* grown in L-Trp-containing medium activated an AhR reporter cell line, whereas supernatants from *L. johnsonii* or *L. murinus* did not (Fig. 4A). To determine whether *L. reuteri* induces DP IELs through the release of AhR ligands, we added *L. reuteri* culture supernatants to naïve ovalbumin-specific $CD4^+$ T cells (OTII) stimulated with ovalbumin peptide-pulsed dendritic cells (DCs) with or without TGFβ (12). *L. reuteri* culture supernatant induced $CD8\alpha\alpha^+CD4^+$ T cell differentiation of OTII T cells, as did the AhR agonist 2,3,7,8-tetrachlorodibenzodioxin (TCDD) (Fig. 4B and fig. S4A) but only in the presence of TGFβ. The AhR antagonist CH223191 inhibited $CD8\alpha\alpha^+CD4^+$ T cell differentiation, confirming that the *L. reuteri* supernatant acts through AhR. AhR agonists plus TGFβ were as effective as TGFβ plus retinoic acid and IFN-γ (12, 14) (Fig. 4B). We

also generated a strain of *L. reuteri* lacking a functional aromatic aminotransferase and hence the ability to convert amino acids into indolic AhR ligands (*L. reuteri* ΔArAT) (24, 26). Culture supernatants from *L. reuteri* ΔArAT failed to stimulate the AhR reporter cells (Fig. 4C). Moreover, *L. reuteri* ΔArAT did not induce DP IELs in JAX mice (Fig. 4D), although this strain colonized mice efficiently (fig. S4B).

We next assessed the impact of dietary L-Trp levels in DP IELs development. More DP IELs were observed in CR mice fed a high L-Trp diet (0.48%) than in mice fed standard (0.24%) or low (0.11%) L-Trp diets (Fig. 4E). However, a high L-Trp diet failed to induce DP IELs in germ-free mice mono-colonized with either *L.reuteri* 100-23 or *L. reuteri* ΔArAT (fig. S4C). Thus, *L. reuteri* acts together with a complex microbiota and dietary L-Trp to induce DP IELs. Bioactivity-guided fractionation of *L. reuteri* 100-23 supernatant identified the presence of indole-3-lactic (ILA) acid, an indole derivative of L-Trp, that activated the AhR reporter cell line and induced CD8αα$^+$CD4$^+$ T cells (fig. S5). This compound was as effective as indole-3-aldehyde (IAId), which activates AhR in ILC3s (24) (Fig. 4F and fig. S4D). *AhR*$^{-/-}$ mice lacked DP IELs, whereas these cells were present in *Ahr*$^{+/-}$ littermates and WT controls supporting our observation that *L. reuteri* induces DP IELs through the release of AhR ligands (Fig. 4G). We next asked whether AhR drives DP IEL differentiation in a T cell intrinsic or extrinsic fashion. TGFβ with either *L. reuteri* culture supernatant or TCDD induced CD8αα$^+$CD4$^+$ T cells from naïve WT CD4$^+$ T cells stimulated in vitro with *AhR*$^{-/-}$ or WT splenic DCs pulsed with a combination of three superantigens. In contrast, *AhR*$^{-/-}$ T cells did not differentiate into CD8αα$^+$CD4$^+$ T cells, whether or not DCs lacked AhR, implying that AhR is required in T cells (Fig. 4H). Moreover, stimulation of OTII T cells with *Ahr*$^{-/-}$ or WT DCs in the presence of TGFβ and either *L. reuteri* supernatant or TCDD induced CD8αα$^+$CD4$^+$ T cells (fig. S4E). Finally, DP IELs were significantly reduced in *Ahr*$^{fl/fl}$ × *Rorc-Cre* mice (which lack AhR in T cells and ILCs), as well as in *Ahr*$^{fl/fl}$ × *Cd4-Cre* mice, (which lack AhR in T cells) in comparison to littermate controls (Fig. 4I, fig. S4 F and G), demonstrating that DP IEL-development requires AhR activation in T cells. To determine when AhR signaling intervenes in the DP IEL-developmental pathway, we analyzed the expression of Thpok in IELs from *Ahr*$^{+/-}$ and *AhR*$^{-/-}$ mice. Thpok^{hi} CD8αα$^-$CD4$^+$ IELs, ThpoK^{lo} CD8αα$^+$CD4$^+$ IELs (DP IELs) and a small intermediate population of ThpoK^{lo} CD8αα$^-$CD4$^+$ IELs were evident in *Ahr*$^{+/-}$ mice, whereas a single Thpok^{hi} CD4$^+$ IEL population predominated in *AhR*$^{-/-}$ mice (Fig. 4J). Thus, lack of AhR signaling arrests DP IEL-development before Thpok downregulation occurs.

Our study reveals that *L. reuteri* provides indole-derivatives of dietary L-Trp, such as indole-3-lactic acid, that activate AhR and lead to downregulation of Thpok and reprogramming of CD4$^+$ IELs into DP IELs. Other indole derivatives may have a similar effect. This Ahr-mediated mechanism is distinct from those by which AhR impacts other T cells with regulatory functions (Tr1, Tregs), intraepithelial γδ T cells and DCs (27–32). Yet undefined microbial species, dietary and/or self-antigens are necessary to expand the CD4$^+$ IEL population with a diverse TCR repertoire that converts into DP IELs. The complete reliance of DP IELs on a single species, *L. reuteri*, and its tryptophan metabolites for their final maturation may provide a basis for the use of *L. reuteri* as a probiotic and tryptophan-

rich food to treat disorders that may be modifiable by DP IELs, such as inflammatory bowel diseases (11).

Supplementary Material

Refer to Web version on PubMed Central for supplementary material.

Acknowledgments

We want to thank Maria Karlsson and David O'Donell for their assistance in the gnotobiotic facility and Jessica Hoisington-Lopez from the DNA Sequencing Innovation Lab at The Edison Family Center for Genome Sciences and Systems Biology for her sequencing expertise. We thank members of our laboratory, in particular Jennifer Bando, for her suggestions and critical reading of this manuscript. This work was supported by the Rainin foundation, U01 AI095542 and DK103039 (M. Colonna), RO1-DK094995 and Burroughs Wellcome Fund (C.S. Hsieh), RO1 CA176695 (M. Cella), DK30292 (J.I. Gordon), and NIH Director's New Innovator Award ID: 1DP2AI124441 (M.S. Donia). P.P.Ahern is the recipient of a Sir Henry Wellcome Postdoctoral fellowship (096100). L. Cervantes-Barragan was supported by Swiss National Science Foundation (fellowship PBSKP3-134332) and the Swiss Foundation for Medical-Biological Grants (fellowship PASMP3-145751).

References and Notes

1. Hooper LV, Littman DR, Macpherson AJ. Interactions between the microbiota and the immune system. Science. 2012; 336:1268–1273. [PubMed: 22674334]
2. Caballero S, Pamer EG. Microbiota-mediated inflammation and antimicrobial defense in the intestine. Annual review of immunology. 2015; 33:227–256.
3. Rooks MG, Garrett WS. Gut microbiota, metabolites and host immunity. Nature reviews. Immunology. 2016; 16:341–352.
4. Ivanov, et al. Induction of intestinal Th17 cells by segmented filamentous bacteria. Cell. 2009; 139:485–498. [PubMed: 19836068]
5. Atarashi K, et al. Induction of colonic regulatory T cells by indigenous Clostridium species. Science. 2011; 331:337–341. [PubMed: 21205640]
6. Atarashi K, et al. Treg induction by a rationally selected mixture of Clostridia strains from the human microbiota. Nature. 2013; 500:232–236. [PubMed: 23842501]
7. Mazmanian SK, Liu CH, Tzianabos AO, Kasper DL. An immunomodulatory molecule of symbiotic bacteria directs maturation of the host immune system. Cell. 2005; 122:107–118. [PubMed: 16009137]
8. Round JL, Mazmanian SK. Inducible Foxp3+ regulatory T-cell development by a commensal bacterium of the intestinal microbiota. Proceedings of the National Academy of Sciences of the United States of America. 2010; 107:12204–12209. [PubMed: 20566854]
9. Sokol H, et al. Faecalibacterium prausnitzii is an anti-inflammatory commensal bacterium identified by gut microbiota analysis of Crohn disease patients. Proceedings of the National Academy of Sciences of the United States of America. 2008; 105:16731–16736. [PubMed: 18936492]
10. Cheroutre H, Husain MM. CD4 CTL: living up to the challenge. Seminars in immunology. 2013; 25:273–281. [PubMed: 24246226]
11. Sujino T, et al. Tissue adaptation of regulatory and intraepithelial CD4(+) T cells controls gut inflammation. Science. 2016; 352:1581–1586. [PubMed: 27256884]
12. Reis BS, Rogoz A, Costa-Pinto FA, Taniuchi I, Mucida D. Mutual expression of the transcription factors Runx3 and ThPOK regulates intestinal CD4(+) T cell immunity. Nature immunology. 2013; 14:271–280. [PubMed: 23334789]
13. Mucida D, et al. Transcriptional reprogramming of mature CD4(+) helper T cells generates distinct MHC class II-restricted cytotoxic T lymphocytes. Nature immunology. 2013; 14:281–289. [PubMed: 23334788]

14. Reis BS, Hoytema van Konijnenburg DP, Grivennikov SI, Mucida D. Transcription factor T-bet regulates intraepithelial lymphocyte functional maturation. Immunity. 2014; 41:244–256. [PubMed: 25148025]
15. Yang Y, et al. Focused specificity of intestinal TH17 cells towards commensal bacterial antigens. Nature. 2014; 510:152–156. [PubMed: 24739972]
16. Hsieh CS, et al. Recognition of the peripheral self by naturally arising CD25+ CD4+ T cell receptors. Immunity. 2004; 21:267–277. [PubMed: 15308106]
17. Pacholczyk R, et al. Nonself-antigens are the cognate specificities of Foxp3+ regulatory T cells. Immunity. 2007; 27:493–504. [PubMed: 17869133]
18. Telesford KM, et al. A commensal symbiotic factor derived from Bacteroides fragilis promotes human CD39(+)Foxp3(+) T cells and Treg function. Gut microbes. 2015; 6:234–242. [PubMed: 26230152]
19. Smith PM, et al. The microbial metabolites, short-chain fatty acids, regulate colonic Treg cell homeostasis. Science. 2013; 341:569–573. [PubMed: 23828891]
20. Arpaia N, et al. Metabolites produced by commensal bacteria promote peripheral regulatory T-cell generation. Nature. 2013; 504:451–455. [PubMed: 24226773]
21. Furusawa Y, et al. Commensal microbe-derived butyrate induces the differentiation of colonic regulatory T cells. Nature. 2013; 504:446–450. [PubMed: 24226770]
22. Walter J, Britton RA, Roos S. Host-microbial symbiosis in the vertebrate gastrointestinal tract and the Lactobacillus reuteri paradigm. Proceedings of the National Academy of Sciences of the United States of America. 2011; 108(Suppl 1):4645–4652. [PubMed: 20615995]
23. Thomas CM, et al. Histamine derived from probiotic Lactobacillus reuteri suppresses TNF via modulation of PKA and ERK signaling. PloS one. 2012; 7:e31951. [PubMed: 22384111]
24. Zelante T, et al. Tryptophan catabolites from microbiota engage aryl hydrocarbon receptor and balance mucosal reactivity via interleukin-22. Immunity. 2013; 39:372–385. [PubMed: 23973224]
25. Schiering C, et al. Feedback control of AHR signalling regulates intestinal immunity. Nature. 2017; 542:242–245. [PubMed: 28146477]
26. Rijnen L, Bonneau S, Yvon M. Genetic characterization of the major lactococcal aromatic aminotransferase and its involvement in conversion of amino acids to aroma compounds. Appl Environ Microbiol. 1999; 65:4873–4880. [PubMed: 10543798]
27. Apetoh L, et al. The aryl hydrocarbon receptor interacts with c-Maf to promote the differentiation of type 1 regulatory T cells induced by IL-27. Nature immunology. 2010; 11:854–861. [PubMed: 20676095]
28. Li Y, et al. Exogenous stimuli maintain intraepithelial lymphocytes via aryl hydrocarbon receptor activation. Cell. 2011; 147:629–640. [PubMed: 21999944]
29. Quintana FJ, et al. Control of T(reg) and T(H)17 cell differentiation by the aryl hydrocarbon receptor. Nature. 2008; 453:65–71. [PubMed: 18362915]
30. Stockinger B, Hirota K, Duarte J, Veldhoen M. External influences on the immune system via activation of the aryl hydrocarbon receptor. Seminars in immunology. 2011; 23:99–105. [PubMed: 21288737]
31. Wu HY, et al. In vivo induction of Tr1 cells via mucosal dendritic cells and AHR signaling. PloS one. 2011; 6:e23618. [PubMed: 21886804]
32. Murray IA, Patterson AD, Perdew GH. Aryl hydrocarbon receptor ligands in cancer: friend and foe. Nat. Rev. Cancer. 2014; 14:801–814. [PubMed: 25568920]
33. Lathrop SK, et al. Peripheral education of the immune system by colonic commensal microbiota. Nature. 2011; 478:250–254. [PubMed: 21937990]
34. Lee JS, et al. AHR drives the development of gut ILC22 cells and postnatal lymphoid tissues via pathways dependent on and independent of Notch. Nature immunology. 2012; 13:144–151.
35. Song C, et al. Unique and redundant functions of NKp46+ ILC3s in models of intestinal inflammation. The Journal of experimental medicine. 2015; 212:1869–1882. [PubMed: 26458769]
36. Kong Y, Xia Y, Nielsen JL, Nielsen PH. Structure and function of the microbial community in a full-scale enhanced biological phosphorus removal plant. Microbiology. 2007; 153:4061–4073. [PubMed: 18048920]

37. Nielsen HV, et al. The metal ion-dependent adhesion site motif of the Enterococcus faecalis EbpA pilin mediates pilus function in catheter-associated urinary tract infection. MBio. 2012; 3:e00177–00112. [PubMed: 22829678]

38. Ruiz N, Wang B, Pentland A, Caparon M. Streptolysin O and adherence synergistically modulate proinflammatory responses of keratinocytes to group A streptococci. Mol Microbiol. 1998; 27:337–346. [PubMed: 9484889]

39. Lefrancois L, Lycke N. Isolation of mouse small intestinal intraepithelial lymphocytes, Peyer's patch, and lamina propria cells. Current protocols in immunology. 2001 17:IV:3.19:3.19.1–3.19.16.

40. Caporaso JG, et al. Ultra-high-throughput microbial community analysis on the Illumina HiSeq and MiSeq platforms. The ISME journal. 2012; 6:1621–1624. [PubMed: 22402401]

41. Caporaso JG, et al. Global patterns of 16S rRNA diversity at a depth of millions of sequences per sample. Proceedings of the National Academy of Sciences of the United States of America. 2011; 108(Suppl 1):4516–4522. [PubMed: 20534432]

42. Edgar RC. UPARSE: highly accurate OTU sequences from microbial amplicon reads. Nature methods. 2013; 10:996–998. [PubMed: 23955772]

43. Caporaso JG, et al. QIIME allows analysis of high-throughput community sequencing data. Nature methods. 2010; 7:335–336. [PubMed: 20383131]

44. Hsieh CS, Zheng Y, Liang Y, Fontenot JD, Rudensky AY. An intersection between the self-reactive regulatory and nonregulatory T cell receptor repertoires. Nature immunology. 2006; 7:401–410. [PubMed: 16532000]

45. Giudicelli V, Chaume D, Lefranc MP. IMGT/V-QUEST, an integrated software program for immunoglobulin and T cell receptor V-J and V-D-J rearrangement analysis. Nucleic Acids Res. 2004; 32:W435–440. [PubMed: 15215425]

46. Solomon BD, Hsieh CS. Antigen-Specific Development of Mucosal Foxp3+RORgammat+ T Cells from Regulatory T Cell Precursors. J Immunol. 2016; 197:3512–3519. [PubMed: 27671109]

47. Pacholczyk R, et al. Nonself-antigens are the cognate specificities of Foxp3+ regulatory T cells. Immunity. 2007; 27:493–504. [PubMed: 17869133]

48. Matsuda K, et al. Establishment of an analytical system for the human fecal microbiota, based on reverse transcription-quantitative PCR targeting of multicopy rRNA molecules. Appl Environ Microbiol. 2009; 75:1961–1969. [PubMed: 19201979]

49. Kriegel MA, et al. Naturally transmitted segmented filamentous bacteria segregate with diabetes protection in nonobese diabetic mice. Proceedings of the National Academy of Sciences of the United States of America. 2011; 108:11548–11553. [PubMed: 21709219]

50. Denman SE, McSweeney CS. Development of a real-time PCR assay for monitoring anaerobic fungal and cellulolytic bacterial populations within the rumen. FEMS Microbiol Ecol. 2006; 58:572–582. [PubMed: 17117998]

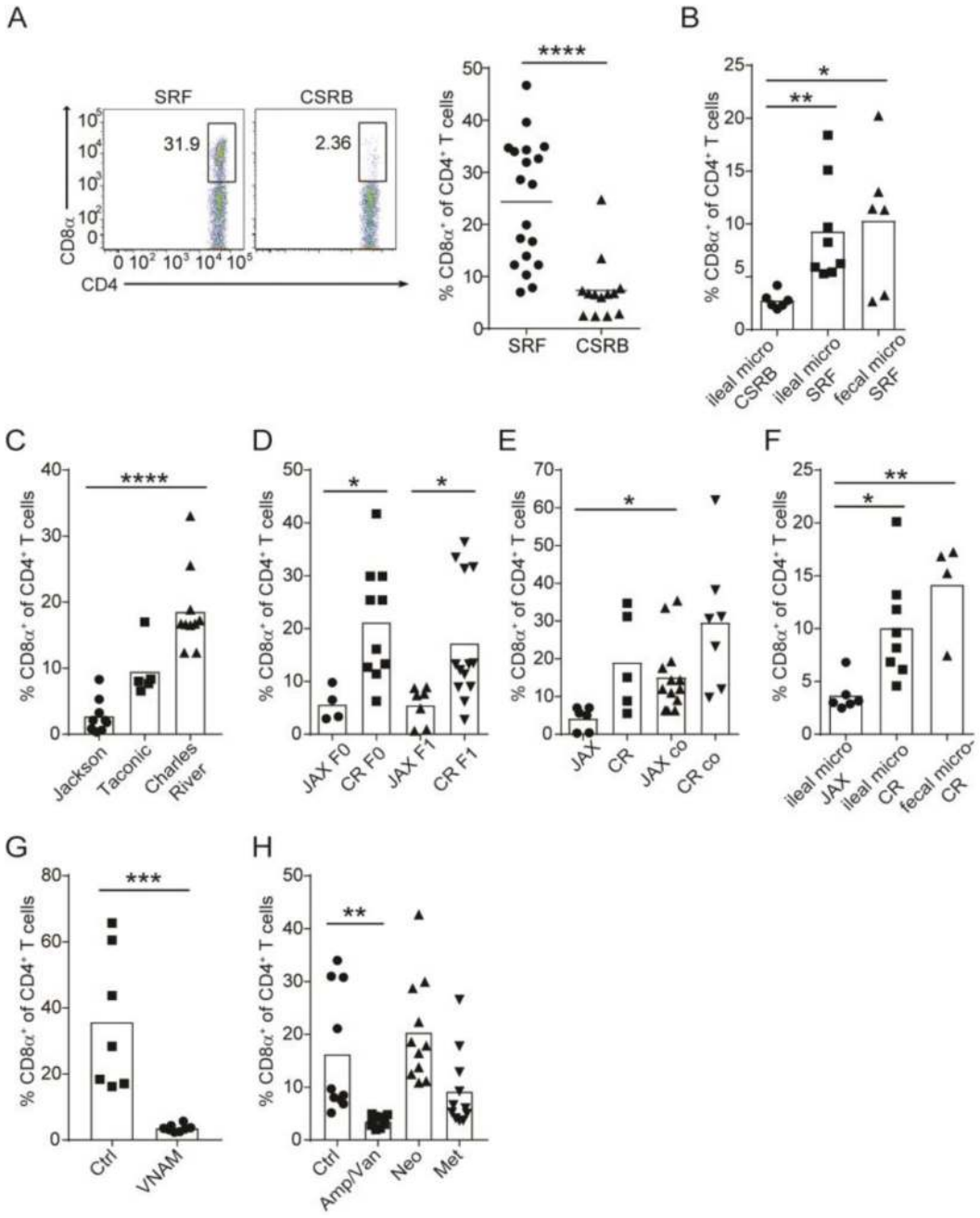

Fig. 1. Specific microbiota components induce DP IELs

(**A**) Representative plots and frequencies of DP IELs (gated on $CD45^+CD3^+TCR\gamma\delta^-CD8\beta^-CD4^+$ IELs) from C57BL/6 mice born in clinical sciences research building (CSRB) and specialized research facility (SRF) facilities. (**B**) DP-IEL frequencies in CSRB mice four weeks after oral gavage with ileal or fecal microbiota harvested from the indicated mice. (**C**) DP-IEL frequencies in C57BL/6 mice from Jackson (JAX), Taconic and Charles River (CR) Laboratories. (**D**) DP-IEL frequencies in F0 and F1 generations of JAX and CR mice bred in CSRB. (**E**) DP-IEL frequencies in JAX or CR mice housed separately (JAX, CR), or cohoused (JAX co, CR co). (**F**) DP-IEL frequencies in JAX

mice treated with ileal or fecal microbiota from the indicated mice. (**G–H**) Frequencies of DP IELs in CR mice that were either untreated (Ctrl), or treated with (**G**) vancomycin, neomycin, ampicillin , and metronidazole (VNAM), or (**H**) ampicillin plus vancomycin (Amp/Van), neomycin (Neo), or metronidazole (Met). Dots represent individual mice. Data are pooled from 2–3 independent experiments. Statistical analysis was performed using Mann−Whitney U test between groups or Kruskal−Wallis test for multiple comparison analysis. (*, $p < 0.05$; **, $p < 0.01$; ***, $p < 0.001$; ****, $p < 0.0001$). Bars represent means.

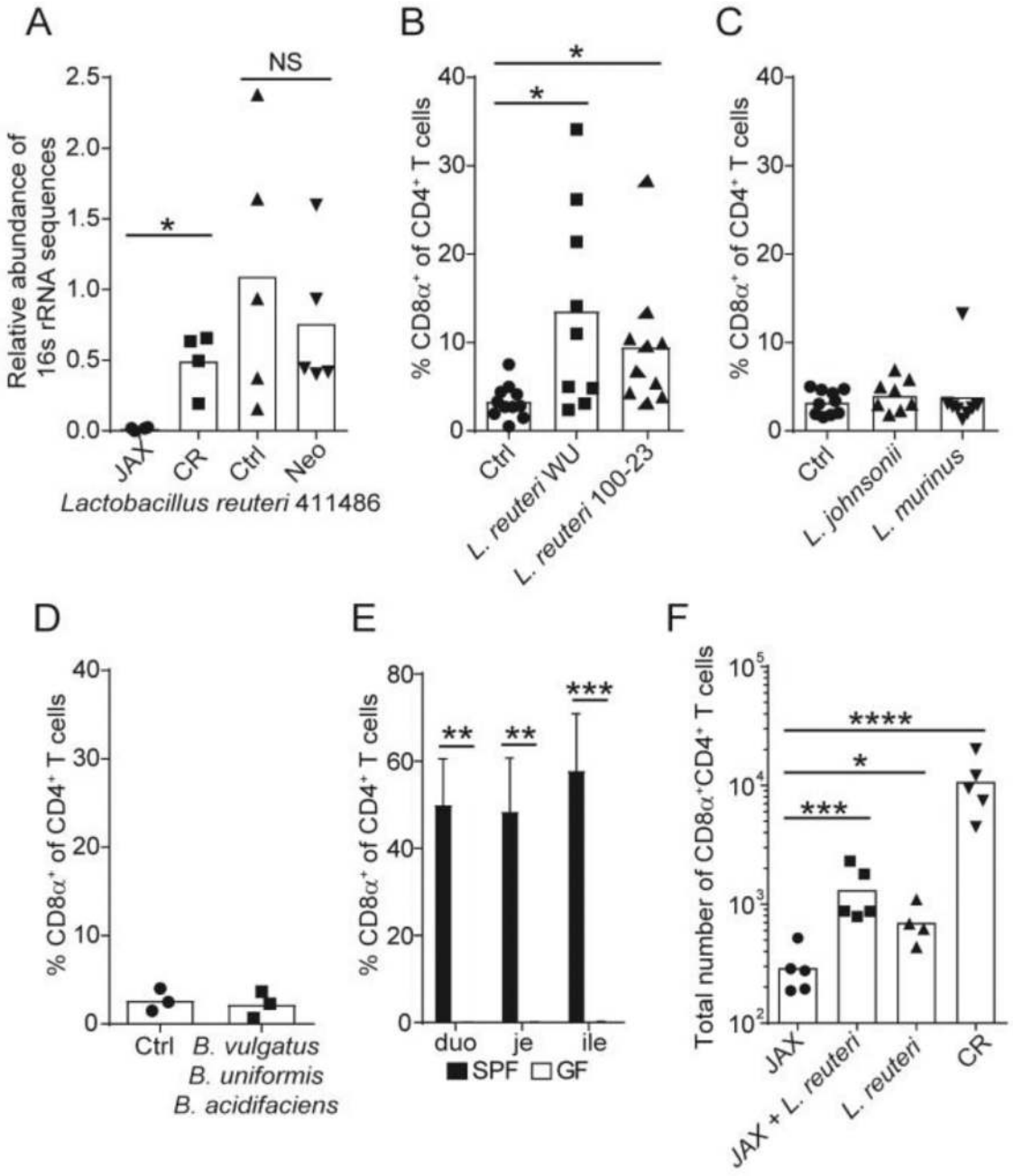

Fig. 2. *L. reuteri* induces DP IELs

(**A**) Relative abundance of *L. reuteri* operational taxonomic unit ID 411486 as determined by sequencing of the V4 region of 16S rRNA genes present in the ileal microbiota of 8-week-old JAX mice and CR mice ($n = 4$); and 4 week-neomycin treated (Neo) or untreated (Ctrl) CR mice (n=5 mice per treatment group). Statistical analysis was performed using Mann −Whitney U test (*, $p < 0.05$). (**B–D**) DP-IEL frequencies in JAX mice colonized with *L. reuteri* WU, *L. reuteri* strain 100-23, *L. johnsonii* WU, *L. murinus*, or a mixture of *Bacteroides vulgatus, B. uniformis*, and *B. acidifaciens*. Untreated JAX mice were used as controls. (**E**) DP IEL-frequencies in specific pathogen free (SPF) and germ-free (GF)

C57BL/6 mice. Duo = duodenum, je = jejunum, ile = ileum. (**F**) Total number of DP IELs in germ-free mice colonized with: JAX mice ileal microbiota; JAX mice ileal microbiota combined with *L. reuteri* W; *L. reuteri* WU alone; or CR ileal microbiota. Dots represent individual mice. Data are pooled from 1–3 independent experiments. Statistical analysis was performed using Mann–Whitney U test between groups or Kruskal–Wallis test for multiple comparison analysis. (*, $p < 0.05$; **, $p < 0.01$; ***, $p < 0.001$; ****, $p < 0.0001$). Bars represent means; error bars represent the SEM.

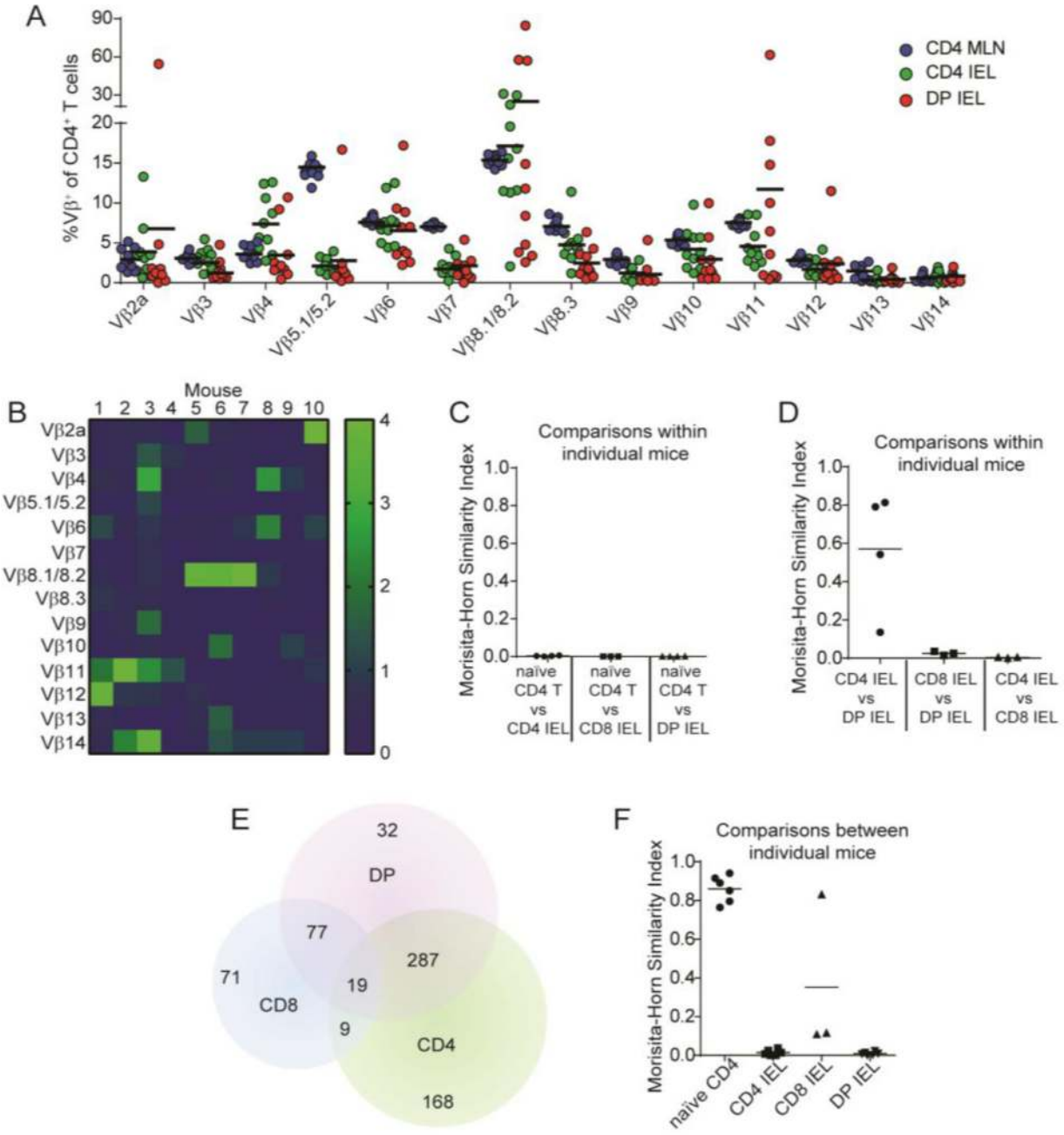

Fig. 3. DP IELs have diverse TCR repertoires in different mice

(**A**) Frequencies of indicated TCR Vβ in DP IELs, CD4 IELs and mesenteric lymph node (MLN) naïve CD4$^+$ T cells from 10 individual DP$^+$ C57BL/6 mice. (**B**) For each TCR Vβ, the ratio between its frequency in DP IELs and its frequency in MLN naïve CD4$^+$ T cells was calculated for individual mice; values are displayed as a heat map. Each column represents a single mouse. (**C–D**) Morisita-Horn similarity analysis of the TCR α-chain repertoires of intraepithelial CD4 IELs, CD8 IELs, DP IELs, and MLN naïve CD4$^+$ T cells. Each symbol represents a comparison between the indicated two subsets within a mouse. Index values of 0 indicate that the two samples are completely dissimilar whereas index

values of 1 indicate that they are indistinguishable. (**E**) Venn diagram showing the number of unique and overlapping complementarity determining region 3 (CDR3) sequences found in TCR α-chains of CD4 IELs, CD8 IELs, and DP IELs. (**F**) Morisita-Horn similarity analysis of the TCR α-chain CDR3 repertoires of CD4 IELs, CD8 IELs, and DP IELs. Each symbol represents a comparison of the TCR-α sequences of the same T cell subset in different mice. Lines indicate mean values. Populations from 4 individual animals were analyzed.

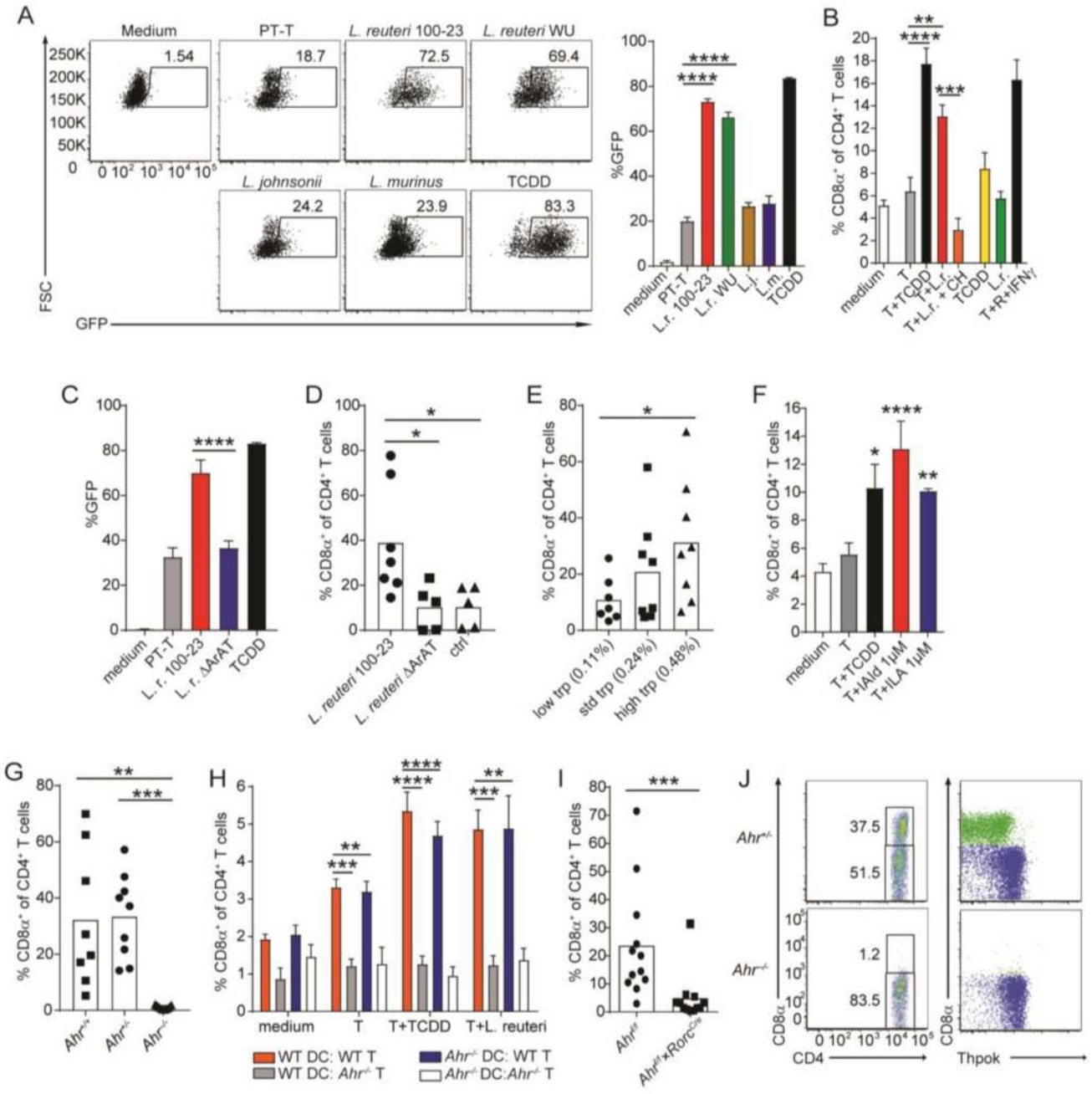

Fig. 4. *L. reuteri* induces DP IELs through AhR activation in T cells

(**A**) Representative plots and quantification of GFP$^+$ cells in an AhR reporter cell line after stimulation with medium (minimum essential medium +10% bovine calf serum), peptone–tryptone water + L-Trp (PT-T), *L.*r., *L. reuteri* WU, *L. reuteri* 100-23; L.j., *L. johnsonii*, or *L.*m., *L. murinus* supernatants (grown in PT-T) or TCDD 2,3,7,8-tetrachlorodibenzodioxin. FSC= Forward Scatter (**B**) CD4$^+$CD8β$^-$CD8α$^+$ T cell frequencies after culture of naïve OTII CD4$^+$ T cells with spleen CD11c$^+$ DCs, $OVA_{329–337}$ peptide, and the indicated stimuli. T = TGFβ; L.r. = *L. reuteri* WU supernatant; CH = CH223191; R = retinoic acid. (**C**) Quantification of GFP$^+$ cells in an AhR reporter cell line after stimulation with medium, PT-

T, *L. reuteri* 100-23 supernatant, *L. reuteri* ΔArAT supernatant, or TCDD. (**D**) DP-IEL frequencies in JAX C57BL/6 mice four weeks after colonization with either *L. reuteri* 100-23, *L. reuteri* ΔArAT, or not colonized (Ctrl). (**E**) DP-IEL frequencies in CR C57BL/6 mice fed for four weeks with low (0.11%), standard (0.24%) or high (0.48%) L-Trp diets. (**F**) $CD4^+CD8\alpha\alpha^+$ T cell frequencies after culture of naïve OTII $CD4^+$ T cells with spleen $CD11c^+$ DCs, $OVA_{329–337}$ peptide, and the indicated stimuli. IAId = indole-3-aldehyde; ILA = indole-3-lactic acid. (**G**) DP-IEL frequencies in cohoused WT, $AhR^{-/+}$ and $AhR^{-/-}$ littermate mice. (**H**) $CD4^+CD8\alpha\alpha^+$ T cell frequencies after culture of WT or $AhR^{-/-}$ $CD4^+$ T cells with WT or $AhR^{-/-}$ DCs, a combination of SEB, SEE, and TSST1 superantigens, and the indicated stimuli. (**I**) DP IEL frequencies in *Rorc-Cre*$^+$ × $Ahr^{fl/fl}$ and *Rorc-Cre*$^-$ × $Ahr^{fl/fl}$ littermates. (**J**) Representative flow cytometry plots showing DP IELs and CD4 IELs (left) and Thpok expression (right) in CD4 IELs (colored blue) and DP IELs (colored green) in $AhR^{-/+}$ and $AhR^{-/-}$ littermates. Dots represent single animals; data have been pooled from 2–3 independent experiments. Statistical analysis was performed using Mann–Whitney U test (**I**), Kruskal–Wallis test (**D, E** and **G**), and One-way ANOVA with Tukey's post hoc test (**A, B, C, F** and **H**) *, $p < 0.05$; **, $p < 0.01$; ***, $p < 0.001$; ****, $p < 0.0001$. Bars represent means, error bars represent SEM.